

Ultra-compact two-dimensional plasmonic nano-ring antenna array for sensing applications

D. Ahmadian · Ch. Ghobadi · J. Nourinia

Received: 12 July 2013 / Accepted: 6 November 2013 / Published online: 30 November 2013
© Springer Science+Business Media New York 2013

Abstract In this paper, a novel optical nanoantenna based on two-dimensional plasmonic nano-ring antenna array is proposed, investigated numerically and compared with a nano-disk antenna array. The results show that the nano-ring structure has resonances similar to the resonances of nano-disk structure but in higher wavelengths. These resonances are tunable by varying the structural parameters of the ring. The optical properties of the proposed structure are investigated in the context of designing a plasmonic refractive index sensor. The nano-ring antenna array sensor has large sensitivity in comparison to the conventional nano-disk antenna arrays. The special feature of the presented structure and the device concepts introduced in this work are applicable in realization of various integrated components and could play an important role in development of plasmonic sensors.

Keywords Surface plasmon · Nanoantenna · Nano-ring array · Refractive index sensor

1 Introduction

Surface plasmon polaritons (SPPs) have been considered as energy carriers to significantly overcome the classical diffraction limit for their ability of confining and propagating the electromagnetic energy in a subwavelength regime (Raether 1988; Barnes et al. 2003).

Among the plasmonic structures, surface plasmon resonance-based nano-scale sensors are very interesting and being used for various applications such as chemical and biological sensing (Haes and Duyne 2002; Alivisatos 2004; Larsson et al. 2007b; Dmitriev et al. 2008), field-enhancement spectroscopies (Aizpurua et al. 2005; Le et al. 2008; Banaee and Crozier 2010; Tripathy et al. 2011), reading DNA bases (Tan et al. 2010), detecting protein-protein interactions (Larsson et al. 2007a; Bukasov et al. 2010), surface membrane binding events (Galush et al. 2009) and antigen-antibody recognition events (Kim et al. 2011).

D. Ahmadian (✉) · Ch. Ghobadi · J. Nourinia
Electrical Engineering Department, Urmia University, 165, 57153 Urmia, Iran
e-mail: davod.ahmadian@gmail.com

The conventional surface plasmon resonance (SPR) sensor has drawbacks in applications due to its bulky system and low spectral resolution (Lee et al. 2009; Svedendahl et al. 2009). On the other hand, localized SPR (LSPR), a coupling between electromagnetic field and spatially confined free-electrons, has a potential for resolving these issues in an attempt to detect nano-scale biological interactions. LSPR sensing structures are normally comprise noble metal nanostructures which are coated on a dielectric substrate. The properties of metallic nanostructures include the optical excitation of LSPRs, enhancement of electric fields, strong localization of the energy at the nanometer scale, and resonance wavelength tunability (Maier 2007; Pelton et al. 2008; Giannini et al. 2010). Since the electron motions determine the resonance condition of LSPR, optical properties of this sensing mechanism are extremely reliant on the geometry of metallic nanostructures. The main issues of the existing LSPR sensor research comprise understanding LSPR characteristics in certain nanostructures, enhancing the design of nanostructures, and improving sensitivity and detection limits.

Nanometer sized rings or ring-like structures have gained significant interest for their favorable properties. Noble metal nano-ring structures were proposed to be used for negative index of refraction (Linden et al. 2004; Zou 2008), wave guiding (Wang and Wang 2006; Bozhevolnyi et al. 2006; Jung et al. 2007), miniature plasmonic wave plates (Drezet et al. 2008), focusing of surface plasmons (Steele et al. 2006; Seo et al. 2007), surface enhanced raman scattering (SERS) (Laurent et al. 2006; Wang et al. 2007; Hao et al. 2007; Clark et al. 2008; Liu et al. 2005; Lu et al. 2005), nanoantennas (Grosjean et al. 2008; Suarez et al. 2007). An on-chip nanosensor has been reported based on the localized surface plasmon resonance property of gold nanorings (Huang et al. 2012; Lodewijks et al. 2012). Such an on-chip nanoring-based biosensor showed a refractive index sensitivity of 350 nm/RIU with a figure of merit of 3.1 and was utilized to detect DNA in a real-time and label-free manner (Huang et al. 2012). Moreover, the plasmonic properties of gold nanorings in close proximity to a gold film have been investigated experimentally to boost near-infrared surface enhanced Raman scattering (SERS) effects. A SERS enhancement factor as large as 1.4×10^7 has been achieved by tuning the separation between the gold nanorings and the gold film (Ye et al. 2010).

In this paper, we propose and demonstrate a plasmonic refractive index sensor based on the nano-ring structure. The finite difference time domain (FDTD) method is employed to simulate and to research its properties. The spectrum and near field distributions for 2D plasmonic nano-ring array have been calculated and compared with conventional nano-disk antenna array. The extremely intense and confined electromagnetic fields induced by the LSPR can realize a highly sensitive sensor to detect small changes in the refractive index of the environment around the nanostructures. Compared with other sensors, the proposed structure has inherent advantages to achieve high integration, high sensitivity, high capability of optimizing the sensing performance, and flexibility in applications.

2 Design

The structures, shown in Fig. 1, comprise a two-dimensional array of gold rings and a two-dimensional array of gold disks of height h_m placed on top of a BK7 glass film with refractive index $n_s = 1.52$. Simulations are performed using the implementation of the finite-difference time-domain (FDTD) method. Figure 1c shows schematic of the computation domain. In all our simulations transmission and reflection spectra were computed for the normal angle of incidence. The dielectric function for gold is approximated using the Drude–Lorentz formula (Shi et al. 2009):

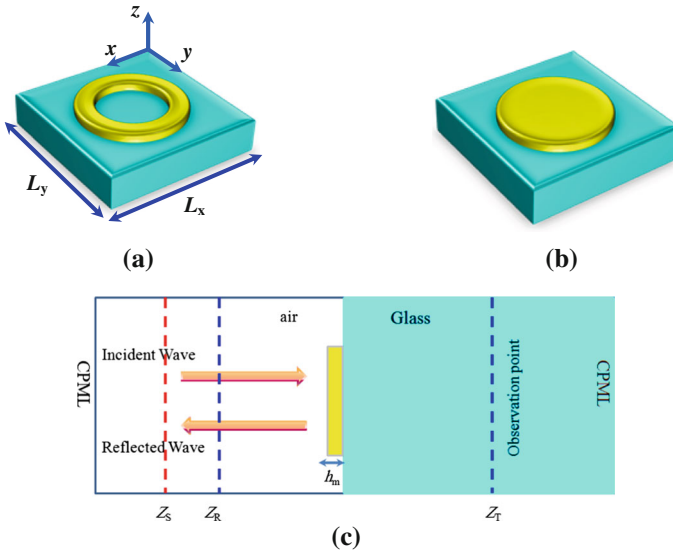


Fig. 1 **a** Single unit cell of a plasmonic nano-ring antenna array. **b** Single unit cell of a plasmonic nano-disk antenna array. **c** General schematic of computational domain

$$\epsilon(\omega) = \epsilon_\infty - \frac{\omega_D^2}{\omega(\omega + i\gamma_D)} - \frac{\Delta\epsilon \cdot \Omega_L^2}{(\omega^2 - \Omega_L^2) + i\Gamma_L\omega} \tag{1}$$

where the dielectric constant at the infinite angular frequency is $\epsilon_\infty = 5.9673$, the bulk plasma frequency $\omega_D = 2\pi \times 2.1136 \times 10^{15}$ rad/s, the damping coefficient $\gamma_D = 2\pi \times 1.592 \times 10^{13}$ rad/s, the oscillator strength $\Omega_L = 2\pi \times 6.5007 \times 10^{14}$ rad/s, the spectral width of the Lorentz oscillators $\Gamma_L = 2\pi \times 1.0486 \times 10^{14}$ rad/s, and the weighting factor $\Delta\epsilon = 1.09$. ω is the angular frequency of the incident electromagnetic radiation.

In the following, the characteristics of the nano-ring antenna array structure are explained by comparing it with the nano-disk antenna array. The single unit cells of the computational domain are shown in Fig. 1a, b, for both structures. For meaningful comparison, the outer dimensions of the both structures are chosen to be the same. The structural parameters of the nano-ring and the nano-disk antenna structures are set as: $h_m = 50$ nm, $L_x = L_y = 500$ nm (lattice period). The values of the ring inner and outer radius are 75 and 100 nm, respectively. The value of the disk radius is 100 nm which is equal to the ring outer radius.

At the faces of a unit cell which are perpendicular to the z direction we impose the convolutional perfectly matched layer (CPML) absorbing boundary conditions. At the remaining four faces (in the x and y directions), we impose periodic boundary conditions. The structure is excited by a modulated Gaussian pulse source (in time) centered around a frequency of interest having a spatial distribution in the form of a plane wave. Incoming plane wave propagates in the air region along $-z$ direction. The electric field of a source is polarized along x direction. The elementary FDTD grid size is $5\text{ nm} \times 5\text{ nm} \times 5\text{ nm}$ in space, and the time step is 0.0094 fs to guarantee numerical stability of simulations. Extent of a unit cell in z direction is 1.5 μm . Extent of a unit cell in the x and y directions are lattice period L_x and L_y . The monitor plane for reflection is located $Z_R = 400$ nm away from the interface between the gold nano-ring or nano-disk and the glass substrate. Source plane is located $Z_S = 600$ nm from the same interface. The monitor surface in the substrate is located $Z_T = 400$ nm away from

the above mentioned interface to calculate the transmission spectrum. In all our simulations the pulse propagated completely through the unit cell after 566 fs.

3 Results and discussion

The transmission and reflection spectra of these structures are calculated and shown in Fig. 2. As shown, the transmission (reflection) spectra of nano-ring and nano-disk antenna array structures have a qualitative similarity: both of them have a transmission minimum (maximum). The transmission minimum of the nano-ring structure has a 3-dB bandwidth of 162 nm centered at the drop-transmission wavelength of $\lambda = 1147$ nm. By comparison, the nano-disk structure has a 3-dB bandwidth of 93 nm centered at drop-transmission wavelength of $\lambda = 808$ nm. Clearly, the 3-dB bandwidth of the transmission drop of the nano-ring antenna array is slightly wider than that of the nano-disk antenna array structure. Moreover, a red-shift of about 339 nm is observed in transmission spectrum of the nano-ring structure with respect to the nano-disk structure. Therefore, the proposed nano-ring structure has all the features of the nano-disk array but in higher wavelengths. As a result, the nano-ring structure can be used as an efficient element in high-integrated optical circuits for miniaturization purpose.

To understand the physics of the plasmon mode in the proposed structures, in Fig. 3 we present the x -component of electric field intensity distribution $|E_x|^2$ in the vicinity of the metal nano-ring and nano-disk at the wavelength of a plasmonic resonance 1,147 nm for the ring structure and 808 nm for the disk structure. In particular, four field distributions are presented: in the xy plane 5 nm above the upper surface of the gold disk/ring (Fig. 3a, e), in the xy plane 5 nm below the lower surface of the gold disk/ring (Fig. 3b, f), in the xz plane (Fig. 3c, g) and in the yz (Fig. 3d, g) plane cut through the center of the gold ring or disk. To ease interpretation of the presented field distributions we note that the structures are illuminated by a plane wave which is polarized in such a way as to contain only the E_x component of the electric field. From Fig. 3, one can see how the plasmons can exhibit the properties of both

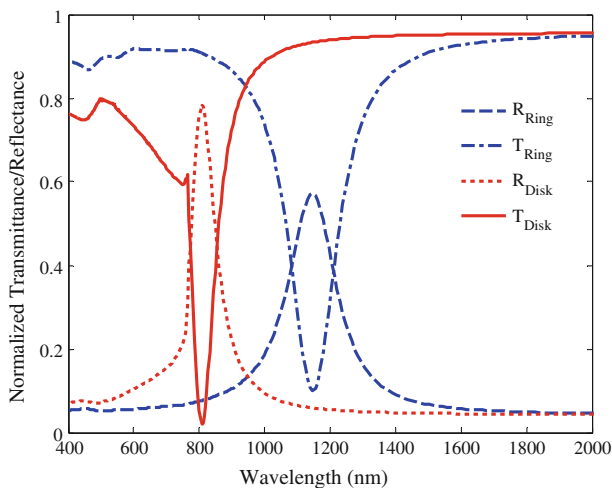


Fig. 2 Comparison of the transmission/reflection spectra of a two-dimensional nano-disk antenna array (*red curves*) and a two-dimensional nano-ring antenna array (*blue curves*). (Color figure online)

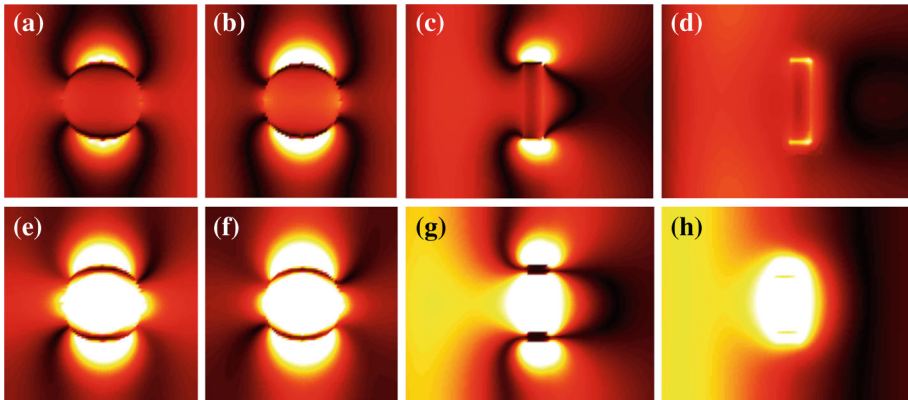


Fig. 3 Distribution of the electric field intensity $|E_x|^2$ in the vicinity of a metal disk/ring at the wavelengths of a plasmon resonance 808 nm for the nano-disk and 1,147 nm for the nano-ring antenna array **a**, **e** xy plane located 5 nm above the upper surface of the gold disk/ring (inside the air), **b**, **f** xy plane located 5 nm below the lower surface of the gold disk/ring (inside the substrate), **c**, **g** xz plane cut through the center of the gold disk/ring, **d**, **h** yz plane cut through the center of the gold disk/ring

long-range and localized plasmons. As can be seen, most of the plasmon energy is strongly localized at the edges of a metallic disk/ring. We can also understand why the width of a plasmon peak in the ring structure is larger than that of the disk structure. Particularly, as the plasmon fields are strongly localized at the ring inner and outer edges, in this respect, the overall plasmon mode of a ring array can be considered as made of the localized plasmons strongly interacting with each other through the field overlap across the boundaries of the adjacent unit cells. However, in the disk structure, the interacting of the plasmon fields of the adjacent disks is weaker than that of the ring structure. As it is well known from the theory of coupled resonator arrays, a narrow eigenstate of a single resonator will be broadened in the resonator array, and such broadening increases with increased interaction between the individual resonators (Shi et al. 2009). Consequently, weaker interaction between the plasmons localized at the individual disks will lead to the narrower resonant states of a disk array.

Successively, we study the effect of the ring inner radius on plasmon resonance. Figure 4a shows the plasmon resonance versus different values of the ring inner radius. In these simulations, we take $R_o = 100$ nm (outer radius of the ring), $L_x = L_y = 500$ nm, and $h_m = 50$ nm. As can be seen, by increasing the value of the ring inner radius from $R_i = 0$ (which is equal to the disk structure) to $R_i = 80$ nm, a red-shift of about 422 nm in plasmon resonance can be observed. From Fig. 4a we note that positions of the plasmon peaks are strongly sensitive to the variation in the ring inner radius size.

In addition, the normalized transmission and reflection of the ring structure versus the value of the ring inner radius are illustrated in Fig. 4b. It is obvious that by increasing the value of the ring inner radius, the transmittance would increase.

Moreover, peak width increases substantially when the inner radius of the ring is increased as shown in Fig. 5. Broadening of the resonance peaks in the case of larger inner radius (lattice constant is fixed) can be rationalized by the stronger inter-cell interaction between the individual plasmons localized at the ring inner edge. This is due to the geometrical fact that more plasmons are localized at the ring edges, when the ring inner radius increases. Consequently, this leads to stronger interaction between the localized plasmons and, hence, spectral broadening of the eigenstates of a ring array.

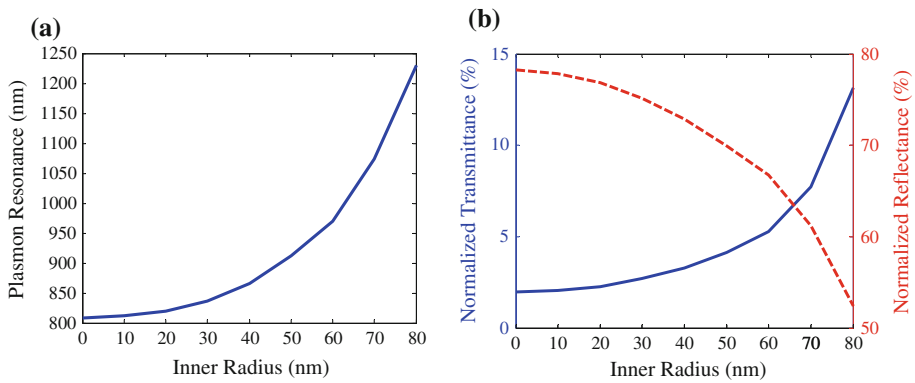


Fig. 4 **a** The plasmon resonance versus different values of the ring inner radius. **b** Normalized transmission/reflection of the nano-ring structure versus the value of the ring inner radius

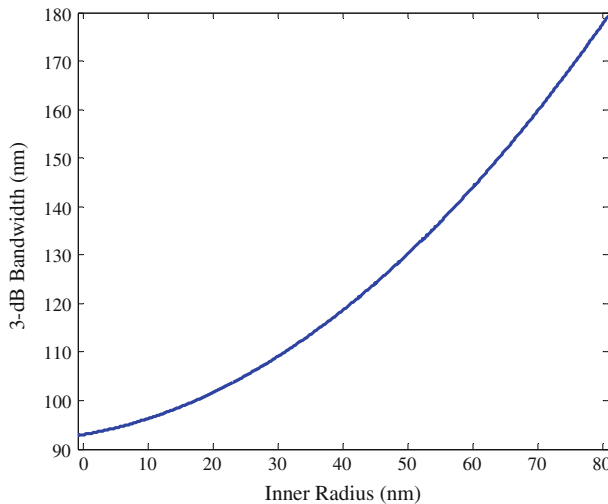


Fig. 5 The plasmonic resonance peak width versus different values of the ring inner radius

According to the simulations and analysis above, it is seen that the proposed nano-ring structure can be easily tuned by changing the ring structural parameters.

One of the important applications of metallic nano-disk and nano-ring antenna arrays is sensing of the refractive index changes in liquid or gaseous analytes. Having fixed the values of the various parameters of the nano-ring array structure, the performance of the proposed devices as plasmonic sensors can now be evaluated. As the main approach to sensing with the proposed structures, we consider spectral detection method. First, one acquires a reflection (or transmission) spectrum for a certain known analyte with a known refractive index. At the same time, one also records spectral positions of the resonant peaks. One then repeats the procedure for a test analyte, extracts positions of the new resonant peaks, and compares them to the positions of the same resonant peaks for a known analyte. Given individual spectral sensitivities of the resonant peaks used in detection, one can then infer the unknown value of test analyte refractive index. Spectral sensitivities of the individual peaks are typically inferred from the calibration measurements, where the refractive index of a known analyte is varied controllably and resonant peak positions are recorded (Shi et al. 2009). Theoretically,

spectral sensitivities of the individual peaks can be evaluated by computing reflection spectra for different values of the analyte refractive index, and then by dividing the value of change in the spectral position of a peak by the value of change in the refractive index of analyte.

The structures of the proposed sensor are the same as Fig. 1. The left side of the structure (Fig. 1c) is filled with the material (liquid or gas) under sensing (MUS). Figure 6a shows the reflection spectra of the nano-disk sensor for different refractive indices. Moreover, the reflection spectra of the nano-ring sensor for different refractive indices, with the same structural parameters as the nano-disk array, are also demonstrated in Fig. 6b. As can be seen from these figures, the reflection maxima wavelength shifts toward long wavelength with the increasing of refractive index of the analyte.

Figure 7 shows that the relationship between the plasmon resonance wavelength and the refractive index of the MUS is a linear function with the sensitivity of $d\lambda/dn = 259$ nm/RIU for the nano-disk structure and $d\lambda/dn = 512$ nm/RIU for the nano-ring structure. Obviously, one can obtain the refractive index (n_a) of the MUS from detecting the plasmon resonance wavelength. Nowadays, a high-resolution optical spectrum analyzer can achieve a wavelength

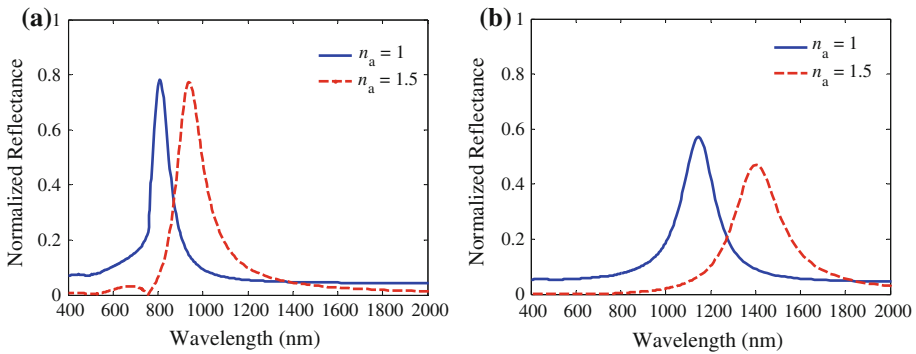


Fig. 6 Normalized reflection spectra of **a** nano-disk antenna array sensor **b** nano-ring antenna array sensor for different refractive indices of materials under sensing

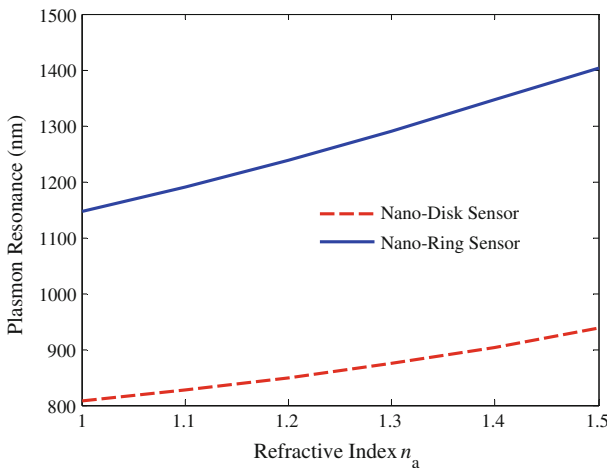


Fig. 7 Plasmon resonance wavelength of the nano-disk and nano-ring antenna arrays versus the analyte refractive index

resolution of $\Delta\lambda = 0.01$ nm. The sensing resolution of the refractive index is defined as minimum detectable refractive index change of the analyte solution: $SR = \Delta\lambda / (d\lambda/dn)$. With the refractive index dispersions in Fig. 7 and the wavelength resolution, the sensing resolution of the refractive index can be achieved to be $SR = 1.9531 \times 10^{-5}$ for the nano-ring structure which is smaller than the corresponding value for the nano-disk structure ($SR = 3.8610 \times 10^{-5}$). Thus, the resolution SR can be enhanced by perforating the nano-disk structure.

An important comparative parameter of sensing devices is the figure of merit (FoM) which takes into account the sharpness of the resonance and thus examines the ability to sensitively measure tiny wavelength changes. We compute the figure of merit of the resonant mode for nano-disk and nano-ring structures via:

$$FoM = \frac{(\partial\lambda_r/\partial n_a)}{FWHM} \quad (2)$$

The FoM of the nano-ring structure is 3.41 which exceeds that of the nano-disk structure (2.73). As can be seen, the refractive index sensitivity and FoM of gold nano-ring structure are larger than those of the nano-disk structure with similar structural parameters. The main reason of the larger refractive index sensitivity of gold nano-ring structure is that a larger fraction of the spatial region with enhanced electric fields is exposed to the material under sensing. As shown in Fig. 3, the electric field is substantially enhanced not only at the outer edges of the ring but also inside the ring cavity. However, for the nano-disk structure, the electric field is enhanced only at the edges of the disk. Moreover, the sensitivity of any plasmonic sensor largely depends on the resonant wavelength. The resonant wavelength of the nano-ring structure is red-shifted with respect to the nano-disk structure. This can be considered as another reason why a nano-ring in general will show a higher sensitivity already compared to a nano-disk structure.

It is also possible to do the sensing by monitoring the variation of the reflected light intensity (I) at a fixed wavelength. The contour maps of the reflected power as a function of the wavelength and the refractive index of the analyte for the nano-disk and nano-ring structures are illustrated in Fig. 8a, b, respectively.

As can be seen, for a fixed wavelength, both structures exhibit a large variation in their reflectance with increasing refractive index of the analyte.

Our simulations demonstrate the feasibility of sensing by using a nano-ring antenna array. Optimization of the structure geometry should lead to improved performance.

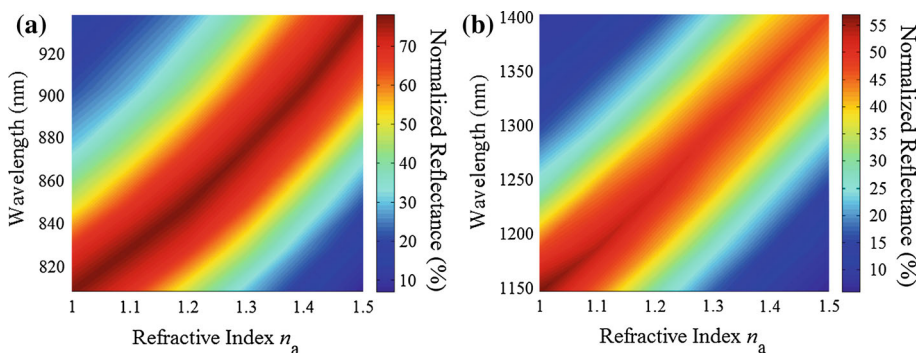


Fig. 8 Contour map of the reflected power of the **a** nano-disk antenna array sensor and **b** nano-ring antenna array sensor as a function of the wavelength and the refractive index of the analyte

4 Conclusion

In this paper, we introduced the plasmonic nano-ring antenna array structure for sensing application. Performance of the proposed structure was characterized and compared with the conventional nano-disk antenna array by FDTD method. It was shown that adding a hollow-core to the conventional nano-disk antenna would shift the transmission spectrum to higher wavelengths, and a nano-ring antenna array is formed. According to the results, the plasmon resonance wavelength in the nano-ring structure is highly tunable by varying the value of the ring inner radius. The resonant mode of the proposed nano-ring antenna array has a sensitivity of 512 nm/RIU (two times greater than the nano-disk array sensor), and a resolution of 1.9531×10^{-5} RIU. The sensing mechanism can be made by monitoring the shift of the resonant wavelength. The proposed structure can be effectively implemented in integrated plasmonics-based optical chips and can be applied to high-resolution biological sensing.

References

- Aizpurua, J., Bryant, G.W., Richter, L.J., García de Abajo, F.J., Kelley, B.K., Mallouk, T.: Optical properties of coupled metallic nanorods for field-enhanced spectroscopy. *Phys. Rev. B* **71**, 235420 (2005)
- Alivisatos, P.: The use of nanocrystals in biological detection. *Nat. Biotechnol.* **22**, 47–52 (2004)
- Banaee, M.G., Crozier, K.B.: Gold nanorings as substrates for surface-enhanced Raman scattering. *Opt. Lett.* **35**, 760–763 (2010)
- Barnes, W.L., Dereux, A., Ebbesen, T.W.: Surface plasmon subwavelength optics. *Nature* **424**, 824–830 (2003)
- Bozhevolnyi, S.I., Volkov, V.S., Devaux, E., Laluet, J.Y., Ebbesen, T.W.: Channel plasmon subwavelength waveguide components including interferometers and ring resonators. *Nature* **440**, 508–511 (2006)
- Bukasov, R., Ali, T.A., Nordlander, P., Shumaker-Parry, J.S.: Probing the plasmonic near-field of gold nanoresonant antennas. *ACS Nano* **4**, 6639–6650 (2010)
- Clark, A.W., Glidle, A., Cumming, D.R.S., Cooper, J.M.: Nanophotonic split-ring resonators as dichroics for molecular spectroscopy. *Appl. Phys. Lett.* **93**, 023121 (2008)
- Dmitriev, A., Hågglund, C., Chen, S., Fredriksson, H., Pakizhev, T., Käll, M., Sutherland, D.S.: Enhanced nanoplasmonic optical sensors with reduced substrate effect. *Nano Lett.* **8**, 3893–3898 (2008)
- Drezet, A., Genet, C., Ebbesen, T.W.: Miniature plasmonic wave plates. *Phys. Rev. Lett.* **101**, 043902 (2008)
- Galush, W.J., Shelby, S.A., Mulvihill, M.J., Tao, A., Yang, P., Groves, J.T.: A nanocube plasmonic sensor for molecular binding on membrane surfaces. *Nano Lett.* **9**, 2077–2082 (2009)
- Giannini, V., Fernández-Domínguez, A.I., Sonnefraud, Y., Roschuk, T., Fernández-García, R., Maier, S.A.: Controlling light localization and light-matter interactions with nanoplasmonics. *Small* **6**, 2498–2507 (2010)
- Grosjean, T., Fahys, A., Suarez, M., Charrat, D., Salut, R., Courjon, D.: Annular nanoantenna on fibre microaxicon. *J. Microsc.* **229**, 354–364 (2008)
- Haes, A.J., Van Duyne, R.P.: A nanoscale optical biosensor: sensitivity and selectivity of an approach based on the localized surface plasmon resonance spectroscopy of triangular silver nanoparticles. *JACS* **124**, 10596–10604 (2002)
- Hao, F., Nordlander, P., Burnett, M.T., Maier, S.A.: Enhanced tunability and linewidth sharpening of plasmon resonances in hybridized metallic ring/disk nanocavities. *Phys. Rev. B* **76**, 245417 (2007)
- Huang, C., Ye, J., Wang, S., Stakenborg, T., Lagae, L.: Gold nanoring as a sensitive plasmonic biosensor for on-chip DNA detection. *Appl. Phys. Lett.* **100**, 173114 (2012)
- Jung, K.Y., Teixeira, F.L., Reano, R.M.: Au/SiO₂ nanoring plasmon waveguides at optical communication band. *J. Lightw. Technol.* **25**, 2757–2765 (2007)
- Kim, D.K., Park, T.J., Tamiya, E., Lee, S.Y.: Label-free detection of leptin antibody–antigen interaction by using LSPR-based optical biosensor. *J. Nanosci. Nanotechnol.* **11**, 4188–4193 (2011)
- Larsson, E.M., Alegret, J., Käll, M., Sutherland, D.S.: Sensing characteristics of NIR localized surface plasmon resonances in gold nanorings for application as ultrasensitive biosensors. *Nano Lett.* **5**, 1256–1263 (2007a)
- Larsson, E.M., Alegret, J., Käll, M., Sutherland, D.S.: Sensing characteristics of NIR localized surface plasmon resonances in gold nanorings for application as ultrasensitive biosensors. *Nano Lett.* **7**, 1256–1263 (2007b)
- Laurent, G., Félijdj, N., Grand, J., Aubard, J., Lévi, G.: Raman scattering images and spectra of gold ring arrays. *Phys. Rev. B* **73**, 245417 (2006)

- Le, F., Brandl, D.W., Urzhumov, Y.A., Wang, H., Kundu, J., Halas, N.J., Aizpurua, J., Nordlander, P.: Metallic nanoparticle arrays: a common substrate for both surface-enhanced Raman scattering and surface-enhanced infrared absorption. *ACS Nano* **2**, 707–718 (2008)
- Lee, B., Roh, S., Park, J.: Current status of micro- and nano-structured optical fiber sensors. *Opt. Fiber Technol.* **15**, 209–221 (2009)
- Linden, S., Enkrich, C., Wegener, M., Zhou, J., Koschny, T., Soukoulis, C.M.: Magnetic response of metamaterials at 100 Terahertz. *Science* **306**, 1351–1353 (2004)
- Liu, G.L., Lu, Y., Kim, J., Doll, J.C., Lee, L.P.: Magnetic nanocrescents as controllable surface-enhanced Raman scattering nanoprobe for biomolecular imaging. *Adv. Mater.* **17**, 2683–2688 (2005)
- Lodewijks, K., Roy, W.V., Borghs, G., Lagae, L., Dorpe, P.V.: Boosting the figure-of-merit of LSPR-based refractive index sensing by phase-sensitive measurements. *Nano Lett.* **12**, 1655–1659 (2012)
- Lu, Y., Liu, G.L., Kim, J., Mejia, Y.X., Lee, L.P.: Nanophotonic crescent moon structures with sharp edge for ultrasensitive biomolecular detection by local electromagnetic field enhancement effect. *Nano Lett.* **5**, 119–124 (2005)
- Maier, S.A.: *Plasmonics: Fundamentals and Applications*. Springer, New York (2007)
- Pelton, M., Aizpurua, J., Bryant, G.: Metal-nanoparticle plasmonics. *Laser Photonics Rev.* **2**, 1–24 (2008)
- Raether, H.: *Surface Plasmons on Smooth and Rough Surfaces and on Gratings*. Springer Tracts in Modern Physics 111, Berlin (1988)
- Seo, S., Kim, H.C., Ko, H., Cheng, M.: Subwavelength proximity nanolithography using a plasmonic lens. *J. Vac. Sci. Technol. B* **25**, 2271–2276 (2007)
- Shi, L., Kabashin, A., Skorobogatiy, M.: Spectral, amplitude and phase sensitivity of a plasmonic gas sensor in a metallic photonic crystal slab geometry: comparison of the near and far field phase detection strategies. *Sens. Actuators B: Chem.* **143**, 76–86 (2009)
- Steele, J.M., Liu, Z., Wang, Y., Zhang, X.: Resonant and non-resonant generation and focusing of surface plasmons with circular gratings. *Opt. Express* **14**, 5664 (2006)
- Suarez, M.A., Grosjean, T., Charrat, D., Courjon, D.: Nanoring as a magnetic or electric field sensitive nano-antenna for near-field optics applications. *Opt. Commun.* **270**, 447–454 (2007)
- Svendahl, M., Chen, S., Dmitriev, A., Kall, M.: Refractometric sensing using propagating versus localized surface plasmons: a direct comparison. *Nano Lett.* **9**, 4428–4433 (2009)
- Tan, Y.N., Su, X., Zhu, Y., Lee, J.Y.: Sensing of transcription factor through controlled-assembly of metal nanoparticles modified with segmented DNA elements. *ACS Nano* **4**, 5101–5110 (2010)
- Tripathy, S., Marty, R., Lin, V.K., Teo, S.L., Ye, E., Arbouet, A., Saviot, L., Girard, C., Han, M.Y., Mlayah, A.: Acousto-plasmonic and surface-enhanced Raman scattering properties of coupled gold nanospheres/nanodisk trimers. *Nano Lett.* **11**, 431–437 (2011)
- Wang, B., Wang, G.P.: Plasmonic waveguide ring resonator at terahertz frequencies. *Appl. Phys. Lett.* **89**, 133106 (2006)
- Wang, S., Pile, D.F.P., Sun, C., Zhang, X.: Nanopin plasmonic resonator array and its optical properties. *Nano Lett.* **7**, 1076–1080 (2007)
- Ye, J., Shioi, M., Lodewijks, K., Lagae, L., Kawamura, T., Dorpe, P.V.: Tuning plasmonic interaction between gold nanorings and a gold film for surface enhanced Raman scattering. *Appl. Phys. Lett.* **97**, 163106 (2010)
- Zou, S.: Light-driven circular plasmon current in a silver nanoring. *Opt. Lett.* **33**, 2113–2115 (2008)